Available online at www.sciencedirect.com
SCIENCE DIRECT
Catalysis Today 98 (2004) 161–170
CATALYSIS TODAY
www.elsevier.com/locate/cattod

Hydroprocessing of dibenzothiophene, 1-methylnaphthalene and quinoline over sulfided NiMo-hydroxyapatite-supported catalysts

Nadia Elazarifi[a], Mohamed Aït Chaoui[a], Abdelhak El Ouassouli[a], Abdelaziz Ezzamarty[a], Arnaud Travert[b], Jacques Leglise[b,1], Louis-Charles de Ménorval[c], Claude Moreau[c,*]

[a]*Laboratoire de Catalyse Hétérogène, Université Hassan II, Faculté des Sciences Aïn Chock, BP 5366, Maarif, Casablanca, Morocco*
[b]*Laboratoire de Catalyse et Spectrochimie, UMR CNRS 6506, ENSICAEN, 6, Bvd du Maréchal Juin, 14050 Caen Cedex, France*
[c]*Laboratoire de Matériaux Catalytiques et Catalyse en Chimie Organique, UMR CNRS 5618, ENSCM, 8, Rue de l'Ecole Normale, 34296 Montpellier Cedex 5, France*

Available online 1 September 2004

Abstract

Hydroprocessing of dibenzothiophene, 1-methylnaphthalene and quinoline was studied in a batch reactor at 340 °C and 7 MPa H_2, over sulfided $NiO–MoO_3$ catalysts supported on calcium-deficient hydroxyapatite materials, enriched or not with Al ions, and aluminium phosphate $AlPO_4$.

On those catalysts, reaction schemes for hydrodesulfurization of dibenzothiophene, hydrogenation of 1-methylnaphthalene and hydrodenitrogenation of quinoline were found to be similar to those already reported for sulfided NiMo catalysts supported on γ-alumina. However, the catalytic activity was significantly improved by using calcium-deficient apatites, particularly for the catalyst referred to as NiMo/ACP-1.5 that contains 1.5 wt.% Al ions, although its specific surface area was lower than that of an industrial alumina supported catalyst.

This increase in activity would result from the presence of superficial defects oxygen vacancies and HPO_4^{2-} species, which would ease the dispersion of the NiMo phase. Moreover, the existence of correlations between the reaction rates for hydrodesulfurization of dibenzothiophene, hydrogenation of 1-methylnaphthalene, hydrodenitrogenation of quinoline and reduction of dimethyldisulfide into methanethiol confirm that the nature of the catalytic sites was the same, whatever the chemical reaction concerned, hydrogenation of aromatic rings or hydrogenolysis of C–S, C–N and S–S bonds.

Keywords: Hydrodesulfurization; Hydrodenitrogenation; Hydrogenation; Sulfided phosphate-based catalysts

1. Introduction

With respect to the european regulation concerning air pollution by diesel exhaust, a continuous effort is made to find new catalytic formulations in order to reduce the sulfur content in gas oil.

In recent papers, it has been reported that sulfided NiMo supported on hydroxyapatite-based solids were more efficient catalysts for the selective conversion of dimethyldisulfide into methanethiol as compared to conventional $NiMo/Al_2O_3$ catalysts [1–3]. It was shown, in particular, that the activity was improved when a calcium-deficient apatite was used because superficial HPO_4^{2-} species or surface defects facilitated the dispersion of the NiMo oxidic precursors and then the sulfided catalytic phase. It is thus of interest to assess the activity of those new sulfide catalysts for the conversion of organic compounds that are present in oils.

Over the last 20 years, dibenzothiophene (DBT), or its 4,6-dimethyl derivative, were found to be particularly relevant models that are representative for deep hydrodesulfurization reaction [4–7]. Hydroxyapatites and $AlPO_4$-enriched apatites were then tested as supports of NiMo sulfides in the

* Corresponding author. Tel.: +33 4 67 16 34 59; fax: +33 4 67 16 34 70.
E-mail address: ezzamarty@caramail.com (A. Ezzamarty), Jacques.leglise@industrie.gouv.fr (J. Leglise), cmoreau@cit.enscm.fr (C. Moreau).
[1] Present address: Ministère de la Recherche et des Nouvelles Technologies, DRRT, 2 Rue Grenet Tellier, 51038 Châlons en Champagne, France.

0920-5861/$ – see front matter © 2004 Elsevier B.V. All rights reserved.
doi:10.1016/j.cattod.2004.07.030

hydrodesulfurization of dibenzothiophene. In addition, catalysts were tested in hydrogenation of 1-methylnaphthalene (1-MN) and hydrodenitrogenation of quinoline (Q).

2. Experimental

All supports and catalysts were characterized by elemental analysis, X-ray diffraction, FT-IR spectroscopy, ^{31}P and ^{27}Al MAS-NMR measurements. Characterization data can be found in previous papers by our group [1–3]. Specific surface areas and pore volumes were calculated from the isotherms of nitrogen adsorption/desorption at 77 K.

2.1. Supports

Phosphate supports were prepared by precipitation as previously reported [1–3]. Calcium phosphate was denoted later as CP, $AlPO_4$-enriched apatites as ACP-*x*, where *x* is the weight percentage of Al in the solid calcined at 400 °C, and the aluminium phosphate as AP. Composition of the hydroxyapatite supports, Ca/P ratio, Al molar fraction, specific surface area (S_{BET}), pore volume (V_p) are given in Table 1.

From X-ray diffraction, it was found that the diagrams of the different solids CP and ACP-*x* calcined at 400 °C resembled that of pure hydroxyapatite [8].

From elemental analysis, the Ca/P atomic ratio of the calcium phosphate CP is equal to 1.58 that agrees with a calcium-deficient apatite. The Ca/P ratio of the apatitic component in ACP-0.9 and ACP-1.5 Al-enriched carriers was calculated as 1.56 and 1.57, and was similar to CP, whereas the Ca/P atomic ratio of ACP-3.4 was found to be equal to 1.66. The apatitic phase of this component was thus stoichiometric. It was deduced that the ACP-0.9, ACP-1.5 and ACP-3.4 supports were made up of crystalline apatite and amorphous aluminium phosphate. The presence of the aluminium phosphate phase was confirmed by ^{31}P and ^{27}Al MAS-NMR measurements, in agreement with results reported in the literature [9]. Moreover, a better dispersion of this phosphate phase was observed by ^{27}Al NMR for Al content less than 1.5 wt.%.

The addition of low amounts of aluminium ions at the synthesis stage resulted in an intimate mixture of crystalline apatite and amorphous $AlPO_4$. This leads to important increases in specific surface area and pore volume (Table 1), those data being close to the corresponding parameters observed for γ-alumina.

From FT-IR measurements, it was noticed that the solids referred to as CP, ACP-0.9 and ACP-1.5 displayed a band at 875 cm^{-1} characteristic of HPO_4^{2-} groups of calcium-deficient apatite. This band was not observed in the infrared spectrum of the ACP-3.4 solid in which the apatitic component is stoichiometric. As we have noticed in the infrared spectra of the Al-containing ACP-1.5 and ACP-3.4 solids, there exists a band in the hydroxyl region at 3795 cm^{-1} which intensity increased with the Al content. This band, assigned to AlOH species, also indicates the presence of an amorphous $AlPO_4$ phase together with the apatite phase [1].

2.2. Catalysts

Catalysts were prepared according to the procedures already described in the literature [1–3] in order to obtain a Mo loading of 3.5 atoms/nm^2 and a Ni/(Ni + Mo) atomic ratio of 0.38, and to be in line with the corresponding parameters of industrial catalysts. The catalysts were sulfided at atmospheric pressure using a fixed-bed technique with a gas mixture of 15% H_2S and 85% H_2 by volume. The oxide precursor previously calcined at 400 °C (particle size: 0.2–0.5 mm) was heated in flowing H_2S/H_2 (gas-flow: 66 ml min^{-1}) from room temperature to 400 °C (3 °C min^{-1}) and held at 400 °C for 4 h, then cooled under H_2S/H_2 flow up to 60–80 °C and finally swept with argon.

The characterization of the hydroxyapatite supported NiMo catalysts in their oxide and sulfide state (oxide content, specific surface area, pore volume and sulfidation degree) is given in Table 2.

From the data reported in Table 2, it can be seen that there is no significant change in the specific surface areas and pore volume after impregnation and sulfidation of MoO_3 and NiO oxides, except for the ACP-3.4 solid that contains stoichiometric apatite mixed with amorphous $AlPO_4$.

From the X-rays diagrams of the Mo/NiMo/NiMoS/ACP-*x* catalysts, it was concluded that the sulfided phase is well dispersed on Ca-deficient catalyst up to ACP-1.5. Indeed, with ACP-3.4 as a support, i.e. apatite in stoichiometric form, a ray at $2\theta = 29°$ ($d = 0.31$ nm), characteristic of MoO_3, was found to be present even after sulfidation. This proves that sulfidation of the ACP-3.4 solid was incomplete. Another conclusion is that superficial defects and HPO_4^{2-}

Table 1
Characterization of the hydroxyapatite carriers

Carrier	Composition (g%)			Ca/P* (at./at.)	Al molar, fraction	S_{BET} (m^2 g^{-1})	V_p (cm^3 g^{-1})
	Ca	Al	P				
CP	38.3	0	18.8	1.58	0	83	0.32
ACP-0.9	36.0	0.9	18.8	1.56	0.034	104	0.48
ACP-1.5	36.0	1.5	19.4	1.57	0.060	140	0.54
ACP-3.4	33.8	3.4	18.0	1.66	0.130	194	0.60
AP	0	25.1	24.5	0	1	155	0.91

* P in the apatite phase.

Table 2
Characterization of hydroxyapatite supported NiMo oxidic and sulfided catalysts

Carrier	Oxides				Sulfides		
	NiO (wt.%)	MoO_3 (wt.%)	S_{BET} ($m^2\ g^{-1}$)	V_p ($cm^3\ g^{-1}$)	S_{BET} ($m^2\ g^{-1}$)	V_p ($cm^3\ g^{-1}$)	S/(Ni + Mo) (at./at.)
CP	1.14	2.47	80	0.31	80	0.45	1.36
ACP-0.9	1.84	4.90	101	0.50	83	0.54	1.47
ACP-1.5	2.44	6.66	131	0.49	107	0.54	1.50
ACP-3.4	3.30	8.85	98	0.43	84	0.45	0.63
AP	2.24	5.83	88	0.59	98	0.46	0.52

groups that were evidenced on Ca-deficient material are necessary in order to provide a good dispersion of the Mo oxide. Those superficial defects and surface HPO_4^{2-} groups are grafting sites of oxides. The addition of aluminium ions at the synthesis stage has then a beneficial effect on the texture, which turns to improve the dispersion of the sulfide phase.

2.3. Typical procedure for HDS dibenzothiophene

Experiments were carried out in a 0.3 l magnetically stirred autoclave (Autoclave Engineers type Magne-Drive), operating in a batch mode and equipped with a system for sampling of liquid during the course of the reaction without stopping the agitation.

Typical procedure was as follows: 0.1 M solution of dibenzothiophene +0.05 M of tetradecane (internal standard) in 80 ml of decane (analytical grade) was poured into the autoclave. The sulfided catalyst (≈0.8 g) was then added to this solution. After purging with nitrogen, the temperature was increased until 340 °C. Nitrogen was then removed and hydrogen was introduced at the required pressure (7 MPa). Zero time was taken when the agitation began.

2.4. Analyses

Analyses were performed on a HP 6890 gas chromatograph equipped with a flame ionisation detector using hydrogen as carrier gas, and a HP5 capillary column (30 m length, 0.32 mm diameter, 0.25 μm thickness). Products were identified by comparison with authentic samples and from GC-MS analysis.

Initial reaction rates were deduced from the experimental concentration versus time curves by determination of the slope at the origin. The calculated reaction rate constants depend on the weight of catalyst and are then referred to 1 g of catalyst. Experimental errors on rate constants are estimated to ±15%.

3. Results

3.1. HDS of dibenzothiophene

The reaction scheme generally admitted for the hydrodesulfurization of dibenzothiophene is reported in Scheme 1 [3,7,10,11]. Biphenyl is representative of the direct desulfurization route and cyclohexylbenzene is representative of the hydrogenation route prior to any desulfurization step. The hydrogenolysis versus hydrogenation activity can then be estimated from the initial biphenyl to cyclohexylbenzene products ratio and/or from the reaction rate constants k_1/k_2 ratio.

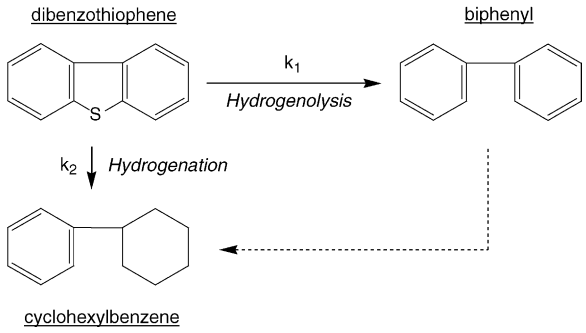

Scheme 1. Simplified reaction scheme for hydrodesulfurization of dibenzothiophene.

In the present work, dibenzothiophene hydrodesulfurization was performed in the absence of H_2S over a series of hydroxyapatite and $AlPO_4$-enriched apatite supported sulfided NiMo catalysts under operating conditions already used in a previous work over an industrial alumina supported NiMo catalyst [10]. Fig. 1 illustrates the reaction profile for hydrodesulfurization of dibenzothiophene in the presence of the sulfided NiMo/ACP-1.5 catalyst. A similar behavior to that already observed for alumina supported NiMo catalysts is observed, i.e. through formation of biphenyl as the major product.

The experimental results obtained over hydroxyapatite and $AlPO_4$-enriched apatite supports are reported in Table 3 together with those of the industrial reference γ-alumina-supported NiMo HR 346 and HR 348 catalysts, the latter containing 2.8 wt.% of phosphorous.

From the results reported in Table 3, it can be seen that the activity is improved, in the absence of hydrogen sulfide in the feed, for the catalysts supported on the calcium-deficient carriers referred to as CP, ACP-0.9 and ACP-3.4 as compared to the industrial HR348 and HR346 reference catalysts. For the sulfided NiMo/ACP-1.5 catalyst, the activity was multiplied by factors of about three and seven compared to HR348 and HR346 catalysts, respectively, although its specific surface area was lower than those of the alumina supported catalysts.

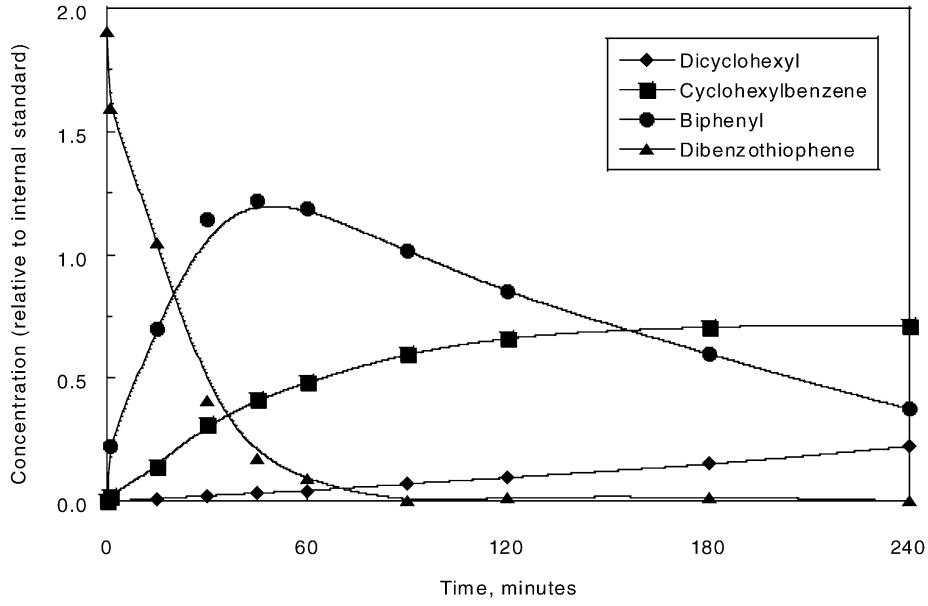

Fig. 1. Concentration vs. time plot for hydrodesulfurization of dibenzothiophene over sulfided NiMo/ACP-1.5 catalyst.

Table 3
Calculated rate constants, $\times 10^2$ min^{-1} (g cata)$^{-1}$, for the disappearance of dibenzothiophene (DBT), and biphenyl vs. cyclohexylbenzene k_1/k_2 ratio, over NiMo catalysts supported on phosphate carriers and over reference NiMo (HR346) and NiMoP (HR348) supported on γ-alumina catalysts (340 °C, 7 MPa H_2, 700 rpm)

Catalyst	k Disappearance DBT	k_1/k_2
HR 348	2.7	4.5
CP	4.1	4.7
ACP-0.9	4.8	4.3
ACP-1.5	7.1	4.3
ACP-3.4	1.3	5.2
AP	1.3	2.2
HR 346	1.1	4.5 [10]

These results closely parallel those obtained in the conversion of dimethyl disulfide into methanethiol [1]. The explanation given was that the presence of superficial HPO_4^{2-} species and related surface defects would facilitate the dispersion of the NiMo phase. No influence of the support is observed on the product distribution, the initial rate constant k_1/k_2 ratio, i.e. hydrogenolysis to hydrogenation ratio, or biphenyl to cyclohexylbenzene ratio, is nearly constant to 4.5, whatever the support, with the exception of the AP-based solid where k_1/k_2 was found to be equal to 2.2. It should also be noted that those values are lower than for the sulfided CoMo catalysts, ≈8.5, on the same carriers [12]. This was expected since CoMo catalysts are known to be more selective for hydrogenolysis than for hydrogenation compared to NiMo catalysts.

3.2. Hydrogenation of 1-methylnaphthalene

The reaction scheme generally admitted for the hydrogenation of 1-methylnaphthalene is reported in Scheme 2.

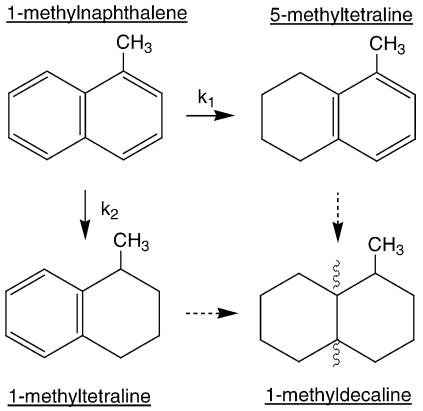

Scheme 2. Simplified reaction scheme for hydrogenation of 1-methylnaphthalene.

Hydrogenation can take place either through the ring bearing the methyl group leading to 1-methyltetraline or through the adjacent benzene ring yielding 5-methyltetraline, the final products being a mixture of *cis* and *trans* 1-methyldecalines.

In the present work, hydrogenation of 1-methylnaphthalene was performed in the absence of H_2S over the same series of hydroxyapatite supported sulfided NiMo catalysts under operating conditions close to those used for hydrodesulfurization of dibenzothiophene (80 ml of a 0.1 M solution of 1-methylnaphthalene in decane, tetradecane as internal standard, 0.8 g of sulfided catalyst, 340 °C, 7 MPa H_2, autoclave 300 ml, 700 rpm). Fig. 2 illustrates the reaction profile for hydrogenation of 1-methylnaphthalene in the presence of the sulfided NiMo catalyst supported on the ACP-1.5 solid with formation of 5-methyltetralin as the major intermediate product.

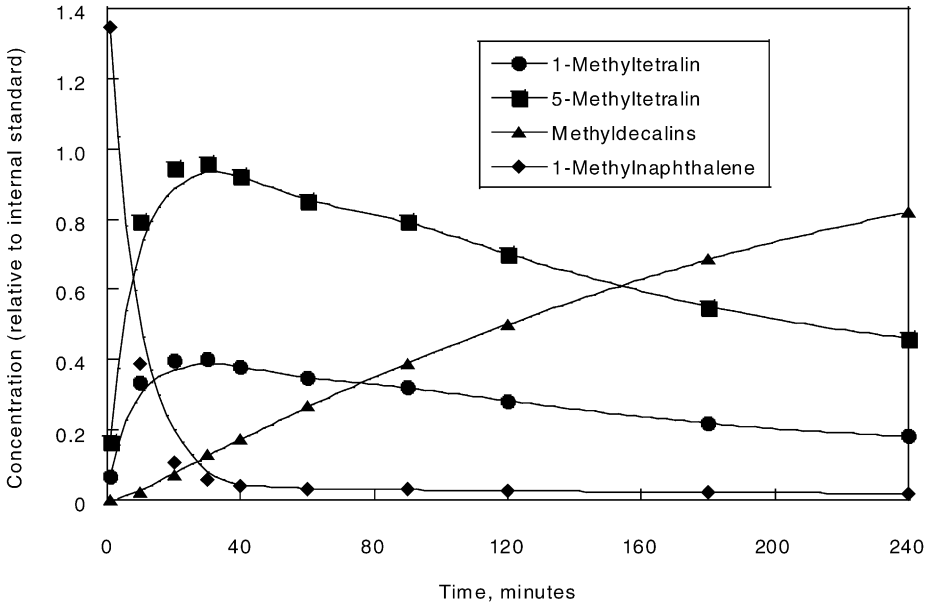

Fig. 2. Concentration vs. time plot for hydrogenation of 1-methylnaphthalene over sulfided NiMo/ACP-1.5 catalyst.

The experimental results obtained over hydroxyapatite supports are reported in Table 4 together with that of the industrial reference HR 348 catalyst.

From the results reported in Table 4, it can be seen that the activity was improved, in the absence of hydrogen sulfide in the feed, for the catalysts supported on the calcium-deficient carriers referred to as CP, ACP-0.9 and ACP-1.5 as compared to the industrial HR348 reference catalyst. For the sulfided NiMo/ACP-1.5 catalyst, the activity was multiplied by a factor of about two, in spite of its lower surface area compared to that of the alumina-supported reference catalyst.

A possible explanation would result from the presence of superficial HPO_4^{2-} species and vacancies, which would facilitate the dispersion of the NiMo phase. No influence of the support was observed on the product distribution, the initial rate constant k_1/k_2 ratio was nearly constant, to about 2.5, whatever the support.

Table 4
Calculated rate constants, $\times 10^2$ min^{-1} (g cata)$^{-1}$, for the disappearance of 1-methylnaphthalene (1-MN), and 5-methyl- to 1-methyltetraline k_1/k_2 ratio, over NiMo catalysts supported on phosphate carriers and over reference NiMoP (HR348) supported on γ-alumina catalyst (340 °C, 7 MPa H_2, 700 rpm)

Catalyst	k Disappearance 1-MN	k_1/k_2
HR 348	4.1	2.3
CP	4.5	2.5
ACP-0.9	5.9	2.0
ACP-1.5	9.9	2.7
ACP-3.4	1.5	2.3
AP	2.1	2.8

3.3. Hydrodenitrogenation of quinoline

The reaction scheme generally admitted for the hydrodenitrogenation of quinoline is reported in Scheme 3. Over alumina supported sulfided NiMo catalysts and in the absence of H_2S, the reaction mainly proceeds through the sequence quinoline → 1,2,3,4-tetrahydroquinoline → decahydroquinoline (DHQ) → propylcyclohexane [13]. In the presence of H_2S or H_2S precursors in the feed, the amount of decahydroquinoline decreases while the amount of ortho-propylaniline increases markedly [14,15].

In the present work, quinoline hydrodenitrogenation was performed in the absence of H_2S over a series of hydroxyapatite supported sulfided NiMo catalysts under operating conditions already used in previous works and exempt from diffusional limitations (80 ml of a 0.1 M solution of quinoline in decane, 0.05 M of dodecane as internal standard, 0.8 g of sulfided catalyst, 0.2–0.5 mm of grain size, 340 °C, 7 MPa H_2, autoclave 300 ml, 700 rpm). Fig. 3 illustrates the reaction profile for the hydrodenitrogenation of quinoline in the presence of the sulfided NiMo/ACP-1.5 catalyst. As already reported for this reaction in the absence of H_2S, the reaction mainly occurs through the rapid formation of 1,2,3,4-tetrahydroquinoline followed by slow hydrogenation of 1,2,3,4-tetrahydroquinoline into decahydroquinoline and fast denitrogenation steps leading to propylcyclohexane as the major final product.

The experimental results obtained over hydroxyapatite supports are reported in Table 5 together with that of the industrial reference NiMoP (HR 348) catalyst.

Examination of Table 5 shows that hydrogenation of quinoline into 1,2,3,4-tetrahydroquinoline was extremely rapid whatever the catalyst carrier. The high reactivity of

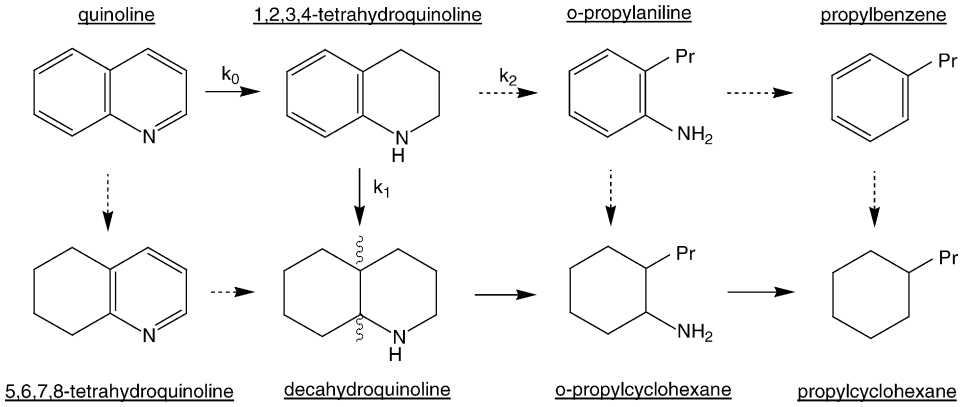

Scheme 3. Simplified reaction scheme for hydrodenitrogenation of quinoline.

quinoline was already attributed to the low aromatic character of the *N*-ring to be hydrogenated [11]. Thus, the hydrodenitrogenation of quinoline is always limited by the disappearance rate of 1,2,3,4-tetrahydroquinoline and, in the absence of hydrogen sulfide in the feed, by that of its nitrogenated intermediate, decahydroquinoline. It should also be added that hydrogenation of 1,2,3,4-tetrahydroquinoline into decahydroquinoline was faster, by a factor of about eight, than its cleavage into orthopropylaniline (OPA). In fact, nitrogen is only completely removed from the fast denitrogenation of propylcyclohexylamine mainly formed from cleavage of DHQ and hydrogenation of orthopropylaniline.

It clearly appears from Table 5 that the sulfided NiMo catalyst supported on the calcium-deficient carrier referred to as ACP-1.5 was the most efficient in the series of hydroxyapatite supported catalysts and was more efficient than the industrial HR348 reference catalyst, by a factor of about two, in spite of its lower surface area.

Table 5
Calculated rate constants, $\times 10^2\ \mathrm{min}^{-1}\ (\mathrm{g\ cata})^{-1}$, for disappearance of quinoline (Q), appearance of decahydroquinoline (DHQ) and orthopropylaniline (OPA) over NiMo catalysts supported on phosphate carriers and over reference NiMoP (HR348) supported on γ-alumina catalyst (340 °C, 7 MPa H_2, 700 rpm)

Catalyst	k_0 Disappearance Q	k_1 Appearance DHQ	k_2 Appearance OPA
HR 348	6	0.47	0.04
CP	21	0.30	0.06
ACP-0.9	23	0.46	0.10
ACP-1.5	36	0.78	0.02
ACP-3.4	14	0.17	0.03
AP	10	0.19	0.06

4. Discussion

All the reactions studied, hydrodesulfurization of dibenzothiophene, hydrogenation of 1-methylnaphthalene and hydrodenitrogenation of quinoline, exhibit high conversion only for NiMo catalysts supported on Ca-deficient and Al-

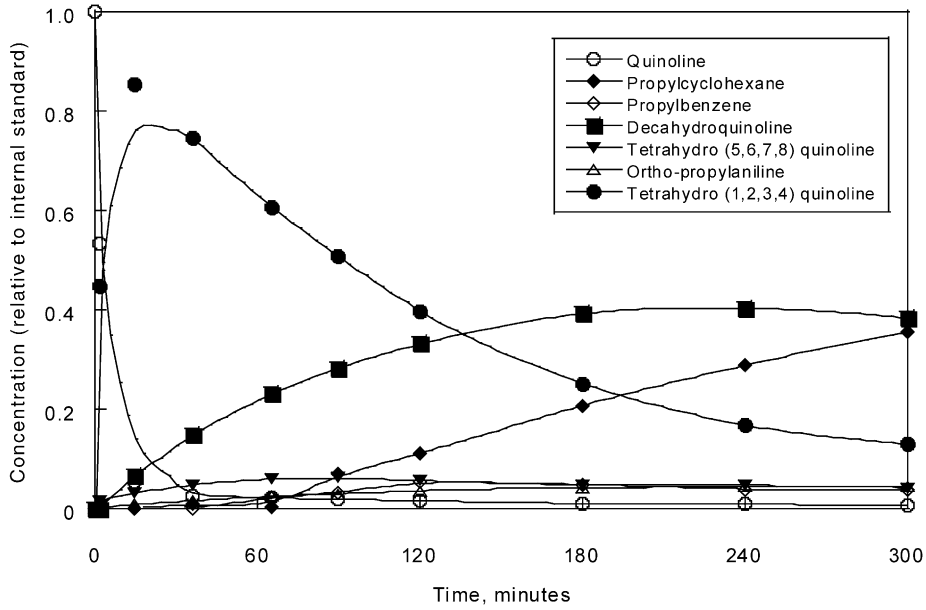

Fig. 3. Concentration vs. time plot for hydrodenitrogenation of quinoline over sulfided NiMo/ACP-1.5 catalyst.

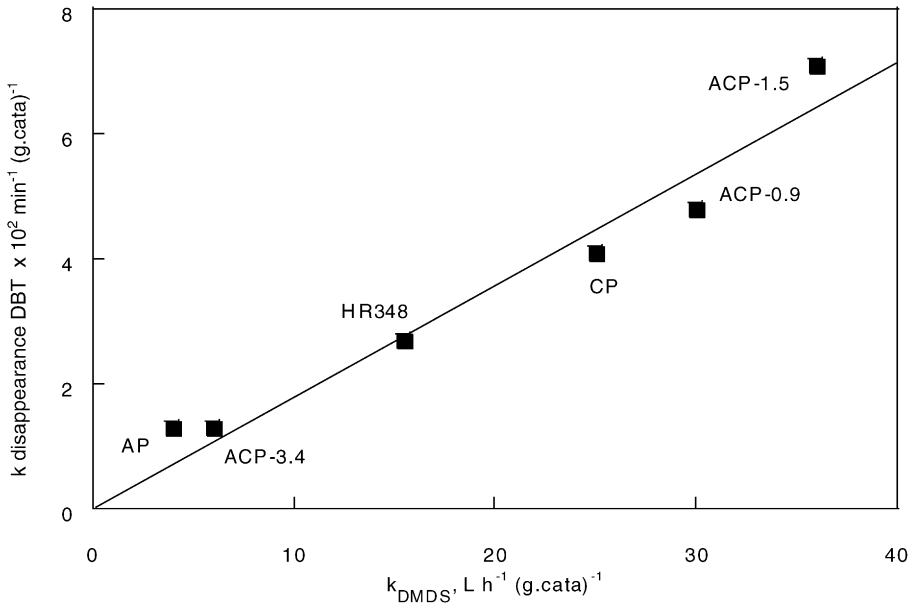

Fig. 4. Dibenzothiophene disappearance rate constants vs. dimethyldisulfide conversion rates for sulfided NiMo supported on Ca-deficient (CP, ACP-0.9, ACP-1.5), stoichiometric (ACP-3.4) and $AlPO_4$ (AP) catalysts.

rich apatites. A similar behavior has already been observed in the conversion of DMDS into methanethiol over the same series of catalysts [1]. It was then interesting to investigate what kind of correlation could exist between all these reactions, which involve hydrogenation of aromatic rings and hydrogenolysis of C–S, C–N and S–S bonds. As illustrated in Figs. 4–8, correlations are found between the rate of conversion of DMDS and (i) the rate of disappearance of dibenzothiophene, which is representative of both hydrogenation and desulfurization routes, (Fig. 4), (ii) the rate of hydrogenation of 1-methylnaphthalene (Fig. 5), (iii) the rate of hydrogenation of quinoline into 1,2,3,4-tetrahydroquinoline (Fig. 6), (iv) the rate of hydrogenation of 1,2,3,4-tetrahydroquinoline into decahydroquinoline (Fig. 7) and (v) the rate of hydrogenolysis of 1,2,3,4-tetrahydroquinoline into orthopropylaniline (Fig. 8).

The calcium phosphate support CP is a Ca-deficient hydroxyapatite with formula $(Ca)_{9.5}(HPO_4)_{0.5}(PO_4)_{5.5}(OH)_{1.5}$. The

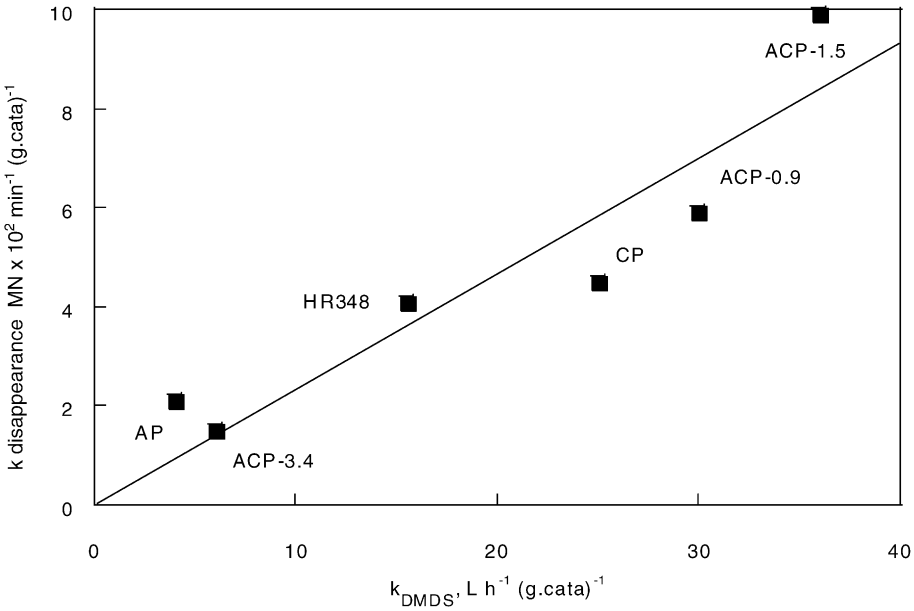

Fig. 5. 1-Methylnaphthalene disappearance rate constants vs. dimethyldisulfide conversion rates for sulfided NiMo supported on Ca-deficient (CP, ACP-0.9, ACP-1.5), stoichiometric (ACP-3.4) and $AlPO_4$ (AP) catalysts.

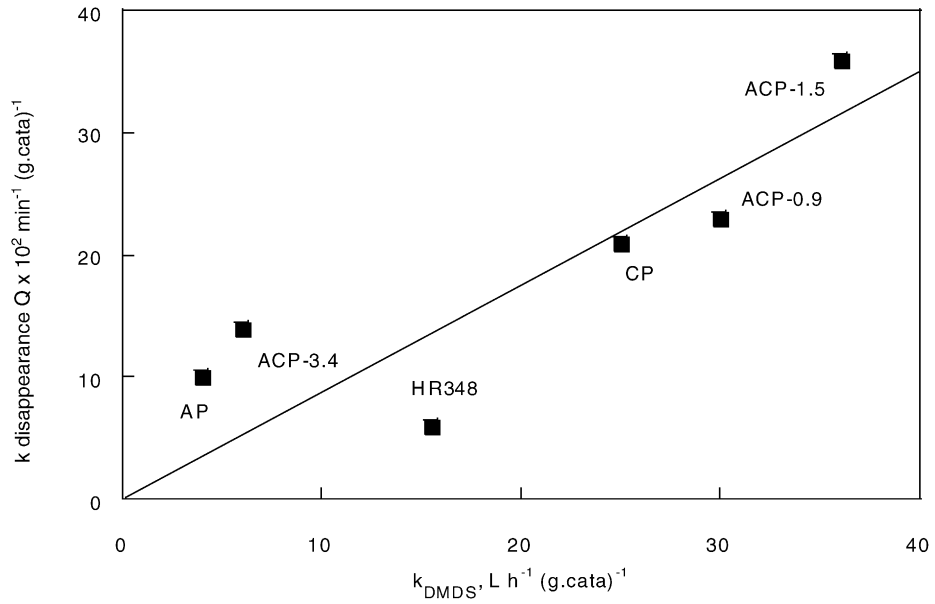

Fig. 6. Quinoline disappearance rate constants vs. dimethyldisulfide conversion rates for sulfided NiMo supported on Ca-deficient (CP, ACP-0.9, ACP-1.5), stoichiometric (ACP-3.4) and $AlPO_4$ (AP) catalysts.

Al-enriched ACP-1.5 and ACP-3.4 samples associate a crystalline apatite with 7 and 15 wt% of amorphous $AlPO_4$ phase, respectively. The amount of amorphous $AlPO_4$ phase may affect the localization of the NiMo phase and consequently the catalytic activity. As shown for DMDS conversion [1], a limit of 3.5 Mo atoms/nm^2 was found for the Ca-deficient hydroxyapatites, CP, ACP-0.9 and ACP-1.5, as well as for the reference NiMo/alumina catalyst, whereas this limit drops to around two Mo atoms per square nanometer for the the stoichiometric ACP-3.4 catalyst containing a relatively important amount of amorphous $AlPO_4$ phase, and, of course for $AlPO_4$ itself, AP. The NiMo phases are better sulfided for the Ca-deficient hydroxyapatites. Moreover, the NiMo/ACP-1.5 catalyst accommodates more NiMo due to its higher surface area (Table 2). The presence of superficial HPO_4^{2-} groups and surface defects then improves the dispersion of the Mo ions in the oxidic precursor, resulting in a better sulfide dispersion and in a better catalytic activity.

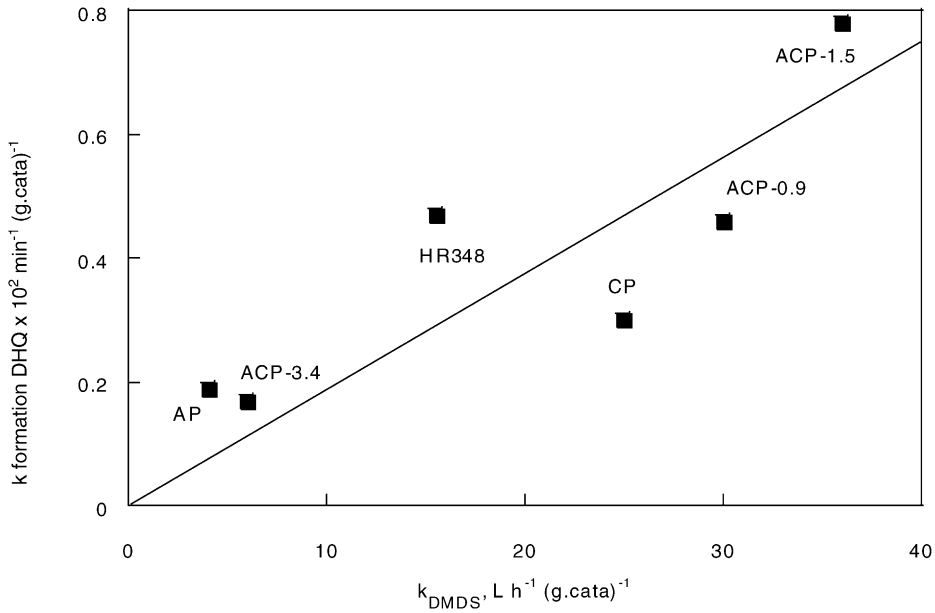

Fig. 7. Decahydroquinoline appearance rate constants vs. dimethyldisulfide conversion rates for sulfided NiMo supported on Ca-deficient (CP, ACP-0.9, ACP-1.5), stoichiometric (ACP-3.4) and $AlPO_4$ (AP) catalysts.

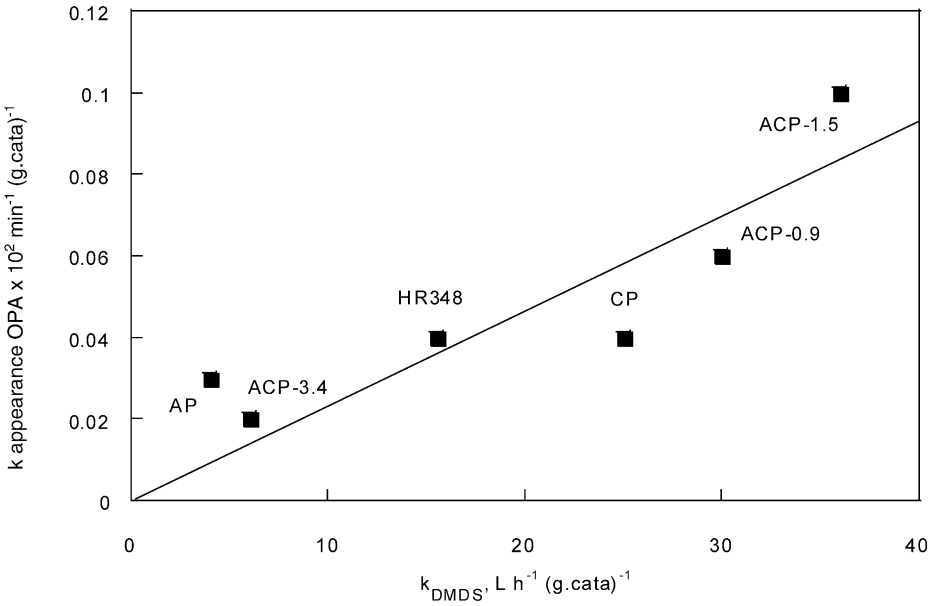

Fig. 8. Orthopropylaniline appearance rate constants vs. dimethyldisulfide conversion rates for sulfided NiMo supported on Ca-deficient (CP, ACP-0.9, ACP-1.5), stoichiometric (ACP-3.4) and $AlPO_4$ (AP) catalysts.

The first consequence of the presence of correlations between hydrodesulfurization, hydrodenitrogenation, hydrogenation and DMDS conversion, is the confirmation of the validity of the different parameters invoked in the conversion of dimethyldisulfide.

The second consequence of the existence of such correlations is that the nature of the catalytic sites, involving protonic and hydride species, is the same whatever the chemical reaction is concerned, hydrogenation of aromatic rings or hydrogenolysis of C–S, C–N and S–S bonds [11,16,17].

5. Conclusion

Hydroxyapatites are efficient supports of sulfided NiMo catalysts for hydrodesulfurization of dibenzothiophene, hydrogenation of 1-methylnaphthalene and hydrodenitrogenation of quinoline. The highest activity is obtained with calcium-deficient catalysts because superficial HPO_4^{2-} species facilitate the dispersion of the NiMo phases. Although their specific surface area is less than for alumina supported catalysts, the apatitic catalysts were found to be more active than the HR348 catalyst used as reference.

In addition, the existence of correlations between the reaction rates of hydrodesulfurization of dibenzothiophene, hydrogenation of 1-methylnaphthalene, hydrodenitrogenation of quinoline and conversion of dimethyldisulfide confirm that the nature of the catalytic sites is the same, whatever the chemical reaction is concerned, hydrogenation of aromatic rings and heterorings or hydrogenolysis of C–S, C–N and S–S bonds. Dimethyldisulfide then appears as a good probe to evaluate the catalytic properties of further hydrotreatment catalysts.

Acknowledgements

The Comité Mixte Interuniversitaire Franco-Marocain is gratefully acknowledged for financial support within the frame of Actions Intégrées N° 97/018/SM and N° MA/02/36.

References

[1] N. Elazarifi, A. El Ouassouli, M. Lakhdar, A. Ezzamarty, J. van Gestel, J. Leglise, Phos. Res. Bull. 10 (1999) 430.
[2] N. Elazarifi, A. El Ouassouli, M. Lakhdar, A. Ezzamarty, L.C. de Ménorval, C. Moreau, J. Lamotte, J. Leglise, in: Proceedings of the 3rd International Meeting on Environment Catalysis and Process Engineering, Fes, Morocco, November, 2000.
[3] N. Elazarifi, A. El Ouassouli, M. Lakhdar, A. Ezzamarty, L.C. de Ménorval, C. Moreau, J. Lamotte, J. Leglise, in: Proceedings of the North American Catalysis Society Meeting, Toronto, Canada, June, 2001.
[4] V. Meille, E. Schulz, M. Lemaire, M. Vrinat, J. Catal. 170 (1997) 29.
[5] V. Meille, E. Schulz, M. Lemaire, M. Vrinat, Appl. Catal. A Gen. 187 (1999) 179.
[6] F. Bataille, J.L. Lemberton, G. Pérot, P. Leyrit, T. Cseri, N. Marchal, S. Kasztelan, Appl. Catal. A Gen. 220 (2001) 191.
[7] J. Leglise, J. van Gestel, L. Finot, J.C. Duchet, J.L. Dubois, Catal. Today 45 (1998) 347.
[8] J.C. Elliott, Structure and Chemistry of the Apatites and Other Calcium Orthophosphates, Elsevier, Amsterdam, 1994.
[9] H. Kraus, R. Prins, J. Catal. 102 (1996) 251.
[10] C. Aubert, R. Durand, P. Geneste, C. Moreau, J. Catal. 97 (1986) 169.

[11] C. Moreau, P. Geneste, in: J.B. Moffat (Ed.), Theoretical Aspects of Heterogeneous Catalysis, Van Nostrand Reinhold, New York, 1990 p. 256.
[12] N. Elazarifi, A. El Ouassouli, A. Ezzamarty, J. Lamotte, J. Leglise, L.C. de Ménorval, C. Moreau, M. Rouimi, M. Ziyad, unpublished results.
[13] C. Moreau, L. Bekakra, A. Messalhi, J.L. Olivé, P. Geneste, Stud. Surf. Sci. Catal. 50 (1989) 107.
[14] S.H. Yang, C.N. Satterfield, Ind. Eng. Chem. Process Des. Dev. 23 (1984) 20.
[15] S. Brunet, G. Pérot, React. Kinet. Catal. Lett. 29 (1985) 15.
[16] J. Leglise, L. Finot, J. van Gestel, J.C. Duchet, Stud. Surf. Sci. Catal. 127 (1999) 51.
[17] C. Calais, M. Lacroix, C. Geantet, M. Breysse, J. Catal. 144 (1993) 160.